

Spatio-Temporal Characteristics of Filamentation in Broad-Area Semiconductor Lasers: Experimental Results

John R. Marciante and Govind P. Agrawal, *Fellow, IEEE*

Abstract— We experimentally study the spatial and temporal characteristics of filamentation in broad-area semiconductor lasers. Near-field measurements show that the spacing between filaments decreases as either the pumping level or the linewidth-enhancement factor is increased. Spectral measurements reveal that spatial filaments are accompanied by periodic or chaotic temporal variations. Our experimental results show excellent qualitative agreement with a theory based on a linear stability analysis of the rate equations for an infinitely wide stripe laser.

Index Terms— Beam filamentation, broad-area lasers, dynamics, laser stability, optical propagation in nonlinear media, semiconductor lasers, spatio-temporal instabilities.

IN THE FIELD of semiconductor lasers, beam filamentation is a critical issue that inhibits their use in high-power applications. The origin of filamentation comes from changes in the carrier density which affect both the optical gain and the refractive index seen by the intracavity field; such index changes are quantified by a parameter known as the linewidth-enhancement factor and denoted by α . As a result, spatial-hole burning induces self-focusing of the optical beam within the semiconductor laser, breaking it up into multiple filaments and limiting the focusable output power of the device. As one might expect, the parameter α governs the extent of filamentation. Numerical simulations indicate that filamentation for broad-area lasers with a stripe width $>50 \mu\text{m}$ occurs if α exceeds 0.5 [1]. Since α typically exceeds 2 for such devices, filamentation is a common problem.

While numerical studies have indicated that spatial filamentation is often accompanied by periodic or chaotic variations of the laser power [2], [3], and a recent analytical model predicts such instabilities [4], the spatio-temporal nature of filamentation in semiconductor lasers has not been extensively studied experimentally. In this letter, we present experimental measurements that show spatial and temporal trends in broad-area semiconductor lasers, and compare these results with theoretical predictions. We also briefly discuss the use of the spatial measurements as a simple technique that can be used for directly comparing the severity of filamentary behavior among different devices.

Manuscript received June 16, 1997; revised September 19, 1997. This work was supported in part by the Army Research Office under the University Research Initiative Program.

J. R. Marciante is with the Air Force Research Laboratory, Directed Energy Directorate, AFRL/DELS, Kirtland AFB, NM 87117-5776 USA.

G. P. Agrawal is with the Institute of Optics, University of Rochester, Rochester, NY 14627 USA.

Publisher Item Identifier S 1041-1135(98)00442-X.

The samples used for the measurements were two sets of quantum-well lasers with $50\text{-}\mu\text{m}$ stripe widths, one set operating at 808 nm and the other at 980 nm. The linewidth enhancement factors for these devices are known to be near $\alpha \approx 4 (\pm 1)$ for AlGaAs lasers operating near 808 nm [5]–[8] and $\alpha \approx 2 (\pm 0.5)$ for InGaAs lasers operating near 980 nm [8]–[11]. Light emitted from the devices was imaged onto a photodiode array to display the near-field profile, from which the spatial information could be extracted. As the injection current was varied, the devices displayed either a multiple-lobed filamentary pattern, noted by deep modulation and the clarity of independent spatial lobes, or exhibited a spatial pattern consisting of several spatial frequencies, resulting in a reduced modulation depth on our slow photodiode array. To ensure that the spatial data was extracted correctly, the injection current was chosen such that the modulation depth of a given filamentation pattern was maximum. In this way, the pump level for which a given spatial pattern dominates could be accurately determined.

In Fig. 1, we plot the dominant filament spacing for the two sets of devices as a function of the pump level r defined as $r = J/J_{\text{th}}$, where J is the injected current density and J_{th} is its value at threshold. The solid lines in Fig. 1 are fit to the experimental data from a previously published theoretical model [4]. Several trends are evident in Fig. 1. First, the filament spacing decreases with increasing pumping level, as has been noted previously [12]. More practically, this means that more filaments fit under the current stripe contact as the current is increased. Since diffractive spreading becomes increasingly stronger as the filament spacing becomes smaller, this observation is a clear indication that increasing the pumping level increases the severity of filamentation. The second trend shown in Fig. 1 is that the filament spacing is smaller for larger values of the linewidth-enhancement factor α . Although lasers fabricated in different material systems generally have parameters that vary somewhat from one another, this second observation is indirect evidence that self-focusing induced by spatial-hole burning is responsible for filamentation. While it is well known that both pumping level and the linewidth-enhancement factor contribute to the increased severity of filamentation, Fig. 1 shows that this increase is directly correlated with a decrease in the filament spacing.

To confirm the spatio-temporal nature of filamentation, one must make temporal or spectral measurements together with the spatial measurements shown in Fig. 1. By splitting off

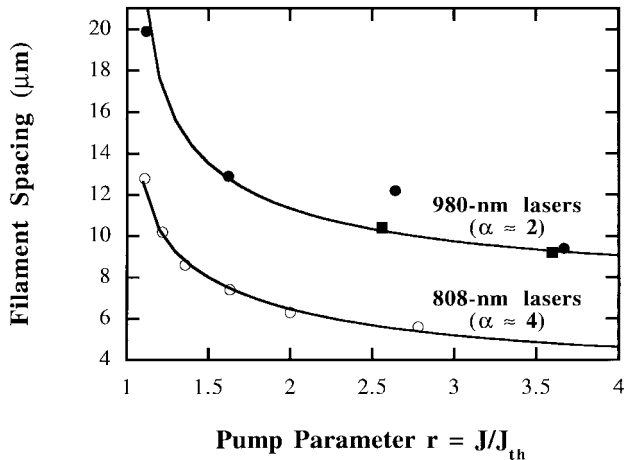


Fig. 1. Measured filament spacing as a function of pump level $r = J/J_{th}$ for 980-nm (solid circles and squares) and 808-nm (empty circles) semiconductor lasers with a $50\text{-}\mu\text{m}$ stripe width. Solid lines are fitted using the theoretical model discussed in the text.

a portion of the light before it was sent to the photodiode array, we measured the spectral properties of the filamented beam. In this branch, the light was sent through astigmatic collimation optics, an isolator, and then finally focused onto a fast photodiode, whose signal was sent to a microwave spectrum analyzer. Any temporal fluctuations in the optical field inevitably lead to relaxation oscillations, resulting in a well-known peak at the relaxation-oscillation frequency Ω_{rel} . However, our measurements show that another frequency was dominant in the intensity noise spectrum of the laser. We refer to this frequency as the filamentation frequency Ω_{fil} . Fig. 2 shows the evolution of the relaxation-oscillation and filamentation frequencies as a function of the pump level for a 980-nm laser. The upper curve was fit to a function of the form $A\sqrt{r-1}$, where A is a fitting parameter, while the lower curve was linearly fit to the experimental data by using the previously published theoretical model [4]. The data indicate that spatial filamentation is accompanied by self-pulsing at a frequency in the 0.5–1.0-GHz range. This periodic modulation of the steady state is a result of the interplay between the nonlinear and diffractive effects that occur during propagation within the semiconductor laser medium.

As discussed earlier, the near field of the laser does not always show well-separated and nearly identical filaments. In these regions, the spectral data does not show a clear indication of Ω_{fil} (shown dashed in Fig. 2). The dashed region for $1 < r < 1.5$ is easily understood by noting that the laser is close enough to threshold and its output power is low enough that α -induced self-focusing has yet to produce filamentation. Near $r = 1.6$, the nonlinear effects become strong enough that the laser enters a self-pulsing regime in which the optical intensity is also spatially modulated. At a pumping level of $r = 2.1$, where the laser displayed a clear, modulated spatial pattern the intensity-noise spectrum showed a narrow peak at the filamentation frequency, accompanied by several harmonics. At pumping level of $r = 2.5$, the laser exhibited a nonperiodic spatial pattern, as described earlier. The intensity-noise spectrum showed multiple peaks, reminiscent of the beating of two frequencies. These observations appear to

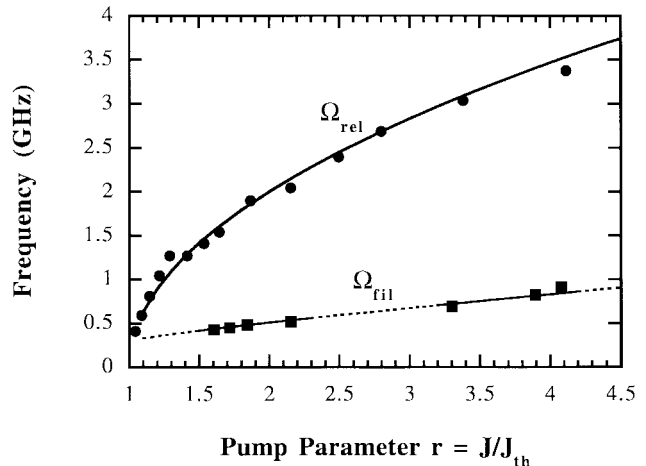


Fig. 2. Measured variation of the relaxation-oscillation and filament frequencies, Ω_{rel} and Ω_{fil} respectively, with the pump level $r = J/J_{th}$ for a 980-nm laser. Solid lines are fitted using the theoretical model discussed in the text.

support the hypothesis that the laser makes a transition toward chaos through a quasiperiodic route. As the pump current was increased beyond this range, the filament frequency re-emerged accompanied by another dominant spatial pattern (i.e., one more filament than was present in the fundamental pattern). For this pumping range, the peak at the filament frequency was rather broad. At a pump level of $r = 4$, the noise spectra showed not only two broad peaks located at Ω_{rel} and Ω_{fil} , but also another broad peak located at $\Omega_{rel}\Omega_{fil}$, in support of our hypothesis of a quasiperiodic route to chaos. Further increase in pump led to a broad-band, nearly featureless spectrum, as would be expected in the chaotic domain.

To understand the experimental data, we make use of a recent model [4] based on the linear stability analysis of the continuous-wave (CW) solution of the underlying dynamic equations which include carrier diffusion, diffraction, and gain saturation (spatial hole burning). Prediction of the spatial properties of filamentation have been made by previous analytic models [2], [13], [14]. The analysis in [14] is only valid for amplifiers, while the laser models neglect either carrier diffusion [13] or propagation of the field in the laser cavity [2]. While the laser model presented in [4] includes both diffusion and propagation, it also allows for temporal modulation of the filaments, a trait not present in any of the previous models yet observable in broad-area semiconductor lasers exhibiting filamentation.

The analytic theory in [4] assumes an infinitely-wide emissive area in the lateral direction, while the lasers we measured had a finite stripe of $50\text{-}\mu\text{m}$ width. As a result, the theory is not likely to provide quantitative agreement but its qualitative predictions should be borne out by our experimental data. The linear stability analysis assumes that a perturbation propagating at a spatial frequency k_x and a temporal frequency Ω becomes unstable under certain conditions and grows exponentially. The growth rate is given in [4] and depends on many parameters such as the pumping level r , the diffusion coefficient of the carriers, the carrier lifetime, and the linewidth-enhancement factor α . Filamentation occurs for values of k_x and Ω for which the growth rate is maximum

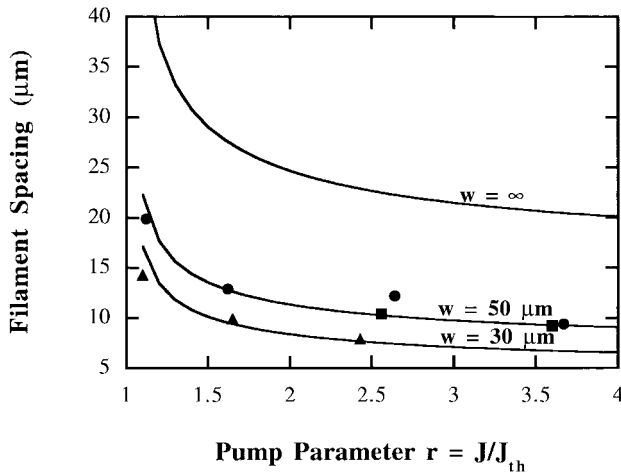


Fig. 3. Measured filament spacing as a function of pump level r for 50- and 30- μm stripe-width lasers ($\alpha \approx 2$), and the theoretical prediction for infinite stripe-width lasers ($\alpha = 2$).

for a given set of laser parameters. By maximizing the growth rate, we can find how the filament spacing $w = 2\pi/k_x$ and the filament frequency $\Omega_{\text{fil}} = \Omega/2\pi$ vary with the pumping level and the linewidth-enhancement factor. The solid lines in Figs. 1 and 2 were obtained by using this model except that the predicted value was linearly scaled to fit the data. The good agreement between theory and experiment shows that the model predicts the correct qualitative behavior in spite of its assumption of an infinitely wide stripe.

The linear scaling needed for a quantitative fit is attributed to the finite stripe width of our lasers. To test this hypothesis further, we performed the same spatial measurements of the dominant filament spacing on a 980-nm laser from the same epitaxial wafer as the other 980-nm lasers, but with a narrower stripe width of 30 μm . The results are displayed in Fig. 3, along with previous measurements of the 50- μm -stripe lasers at 980 nm and theoretical predictions for $\alpha = 2$. From this figure, we see that the effect of a finite stripe width is to squeeze the filaments more tightly together; the narrower the stripe, the more closely spaced the filaments become. Fig. 3 suggests that measurements on a laser with a wide enough current stripe ($>200 \mu\text{m}$) should agree quite well with the theoretical predictions both qualitatively and quantitatively.

It is well known that increasing either the pumping level or the linewidth-enhancement factor α results in a greater degree of filamentation for a broad-area laser. What we have experimentally shown, and what the analytic theory [4] predicts, is that the increase in filamentary behavior causes a decrease in the filament spacing. From a practical point of view, one can use this analysis as a way to compare the severity of filamentation in different devices. Since the reduction in the filament spacing is a direct measure of the filamentary tendencies of the device, a quick and easy measurement of spatial characteristics as presented above can be used to qualitatively compare the severity of filamentation among different semiconductor lasers.

In conclusion, we have experimentally studied the spatial and temporal characteristics of filamentation in broad-area

semiconductor lasers. Near-field measurements show that the spacing between filaments decreases as either the pumping level or the linewidth-enhancement factor is increased. Spectral measurements reveal periodic or chaotic temporal variations and support the hypothesis that the laser makes a transition toward spatio-temporal chaos at high pumping levels. Our experimental results show excellent qualitative agreement with a theoretical model based on a linear stability analysis of the rate equations. We experimentally determined that discrepancies between experiment and theory are due to the finite stripe width of the laser. Since the spatial behavior of the laser can be directly linked to filamentary tendencies, this simple measurement technique can be used to compare the severity of filamentation in different semiconductor lasers.

ACKNOWLEDGMENT

The authors wish to thank G. Wicks and M. Koch for the semiconductor laser samples, and G. van Tartwijk for stimulating and helpful discussions.

REFERENCES

- [1] J. R. Marcianti and G. P. Agrawal, "Nonlinear mechanisms of filamentation in broad-area semiconductor lasers," *IEEE J. Quantum Electron.*, vol. 32, pp. 590–596, 1996.
- [2] H. Adachihiro, O. Hess, E. Abraham, P. Ru, and J. V. Moloney, "Spatiotemporal chaos in broad-area semiconductor lasers," *J. Opt. Soc. Amer. B*, vol. 10, pp. 658–665, 1993.
- [3] O. Hess, S. W. Koch, and J. V. Moloney, "Filamentation and beam propagation in broad-area semiconductor lasers," *IEEE J. Quantum Electron.*, vol. 31, pp. 35–43, 1995.
- [4] J. R. Marcianti and G. P. Agrawal, "Spatio-temporal characteristics of filamentation in broad-area semiconductor lasers," *IEEE J. Quantum Electron.*, vol. 33, pp. 1174–1179, July 1997.
- [5] I. D. Henning and J. V. Collins, "Measurements of the semiconductor laser linewidth broadening factor," *Electron. Lett.*, vol. 19, pp. 927–929, 1983.
- [6] S. S. Lee, L. Figueroa, and R. Ramaswamy, "Variations of linewidth enhancement factor and linewidth as a function of laser geometry in (AlGa)As lasers," *IEEE J. Quantum Electron.*, vol. 25, pp. 862–870, 1989.
- [7] M. P. van Exter, W. A. Hamel, J. P. Woerdman, and B. P. Zeijlman, "Spectral signature of relaxation oscillations in semiconductor lasers," *IEEE J. Quantum Electron.*, vol. 28, pp. 1470–1478, 1992.
- [8] A. Schönfelder, S. Weisser, J. D. Ralston, and J. Rosenzweig, "Differential gain, refractive index, and linewidth enhancement factor in high-speed GaAs-based MQW lasers: Influence of strain and p-doping," *IEEE Photon. Technol. Lett.*, vol. 6, pp. 891–893, 1994.
- [9] W. Rideout, B. Yu, J. LaCourse, P. K. York, K. J. Beernick, and J. J. Coleman, "Measurement of the carrier dependence of differential gain, refractive index, and linewidth enhancement factor in strained-layer quantum well lasers," *Appl. Phys. Lett.*, vol. 56, pp. 706–708, 1990.
- [10] R. Raghuraman, N. Yu, R. Engelmann, H. Lee, and C. L. Shieh, "Spectral dependence of differential gain, mode shift, and linewidth enhancement factor in a InGaAs-GaAs strained-layer single-quantum-well laser operated under high injection conditions," *IEEE J. Quantum Electron.*, vol. 29, pp. 69–75, 1993.
- [11] D. J. Bossert and D. Gallant, "Gain, refractive index, and α -parameter in InGaAs-GaAs SQW broad-area lasers," *IEEE Photon. Technol. Lett.*, vol. 8, pp. 322–324, 1996.
- [12] R. J. Lang, A. G. Larsson, and J. G. Cody, "Lateral modes of broad area semiconductor lasers: Theory and experiment," *IEEE J. Quantum Electron.*, vol. 27, pp. 312–320, 1991.
- [13] D. Mehuys, R. J. Lang, M. Mittelstein, J. Salzman, and A. Yariv, "Self-stabilized nonlinear lateral modes of broad area lasers," *IEEE J. Quantum Electron.*, vol. 23, pp. 1909–1920, 1987.
- [14] A. H. Paxton and G. C. Dente, "Filament formation in semiconductor laser gain regions," *J. Appl. Phys.*, vol. 70, pp. 1–6, 1991.